

ISTITUTO NAZIONALE DI FISICA NUCLEARE
Laboratori Nazionali di Frascati

LNF-85/10(P)
29 Marzo 1985

G. Martinelli:
COLLIDER RESULTS AND QCD PREDICTIONS

Invited talk at the 5th Topical Workshop on Proton-
Antiproton Collider Physics, S. Vincent, Aosta Valley,
Italy - 25 February - 1st March, 1985

COLLIDER RESULTS AND QCD PREDICTIONS

G. Martinelli

INFN, Laboratori Nazionali di Frascati, Italy

ABSTRACT

A comparison of theoretical predictions from perturbative QCD for W and Z^0 production and for jet physics and experimental results at Collider energies is presented.

1. INTRODUCTION

A very important part of the physics explored by the UA1 and UA2 experiments at the CERN Collider concerns QCD. QCD constitutes an important aspect of Collider physics for two main reasons.

Firstly our belief that it describes the physics of strong interactions is not based on a single very precise experimental test, but on the converging agreement (qualitative and/or quantitative) of many different experimental results (accumulated over the last ten years) with theoretical predictions from QCD: the CERN Collider offers a unique possibility of testing QCD in a completely new range of energies.

Secondly QCD processes are the background to new phenomena and accurate quantitative predictions for these processes are needed in order to separate the physics of the Standard model from the signals of a new physics.

The discussion here following is divided into two parts. In Sect. 2 I will discuss QCD effects in W and Z^0 production. For these processes QCD predictions reached a quite high level of accuracy and a

quantitative comparisons of theoretical expectations and experimental results can already be made. In contrast with this particularly favourable case predictions for jet physics are still affected by large theoretical uncertainties and the agreement between theory and experiments can be tested only at a rather qualitative level. The present status of the theory for jet physics will be presented in Sect. 3 together with a discussion intended to point out the aspects that should be further explored in order to reduce theoretical uncertainties.

2. QCD EFFECTS IN W AND Z⁰ PRODUCTION

At the CERN Collider W/Z⁰ production tests the Drell-Yan mechanism in a completely new energy range. Most of theoretical problems encountered at fixed target and ISR energies ($\sqrt{S} \approx 27-63$ GeV) almost disappear. Radiative corrections due to strong interactions for total cross-sections, rapidity and q_T distributions can be reliably computed in perturbative QCD since theoretical uncertainties are relatively small in the present range of center of mass energies ($\sqrt{S} = 540-630$ GeV).

Radiative corrections modify the naive (and leading logarithms improved) parton model predictions for all the interesting measurable quantities:

- 1) Total production cross-section σ^{W,Z^0} *
- 2) Rapidity distribution $(d\sigma^{W,Z^0}/dy)/\sigma^{W,Z^0}$ *
- 3) Charge asymmetry
- 4) Transverse momentum distribution $d\sigma^{W,Z^0}/dq_T$ *
- 5) Transverse energy distribution $d\sigma^{W,Z^0}/dE_T$ *

.
. .
. .
. .

It turned out that the effects of radiative corrections are particularly

important for the quantities denoted by * in the list reported above^(f). Hence I will discuss in the following only the modifications, due to radiative corrections, to the total production cross section and to the q_T and E_T distributions.

2.1 Total W/Z^0 production cross section

In Fig. 1 the lowest order process for W/Z^0 production via Drell-Yan mechanism is shown together with the first order diagrams contributing to the total cross section^(o). The result of the complete first order computation has the simple form^(1,2):

$$\sigma^{W,Z^0} = N_{W,Z^0} \int \frac{dx_1 dx_2}{x_1 x_2} \left\{ \left[H(x_1, x_2, P^2) + (1 \leftrightarrow 2) \right] \right. \\ \left. \left[\delta\left(1 - \frac{\tau}{x_1 x_2}\right) + \frac{2\alpha_s(P^2)}{3\pi} \Theta(x_1 x_2 - \tau) f_q\left(\frac{\tau}{x_1 x_2}\right) \right] + \right. \\ \left. \left[K(x_1, x_2, P^2) + (1 \leftrightarrow 2) \right] \frac{\alpha_s}{4\pi} \Theta(x_1 x_2 - \tau) f_g\left(\frac{\tau}{x_1 x_2}\right) + O(\alpha_s^2) \right\} \quad (1)$$

where $N_{W,Z}$ is a normalization constant and

$$H(x_1, x_2, P^2) \sim q(x_1, P^2) \bar{q}(x_2, P^2)$$

and

$$K(x_1, x_2, P^2) \sim (q(x_1, P^2) + \bar{q}(x_1, P^2)) g(x_2, P^2)$$

are the appropriate bilinear combinations of parton distributions. $f_{q,g}(z)$ are computable kernels (depending on the choice of the scale P^2 for the parton densities) and $\tau = M_{W,Z}^2/S$.

(f) In other cases radiative corrections are much less important. For example the first order corrections sensibly modify $d\sigma/dy$ and σ ("K factors"). However the normalized y distribution $(d\sigma/dy)/\sigma$ is in practice unaffected by these corrections in the experimental accessible range of y .

(o) The order α_s diagrams of Fig. 1 not only correct the naive parton model expectations for the total cross section but are also responsible for the (perturbative) transverse momentum distribution of intermediate vector bosons.

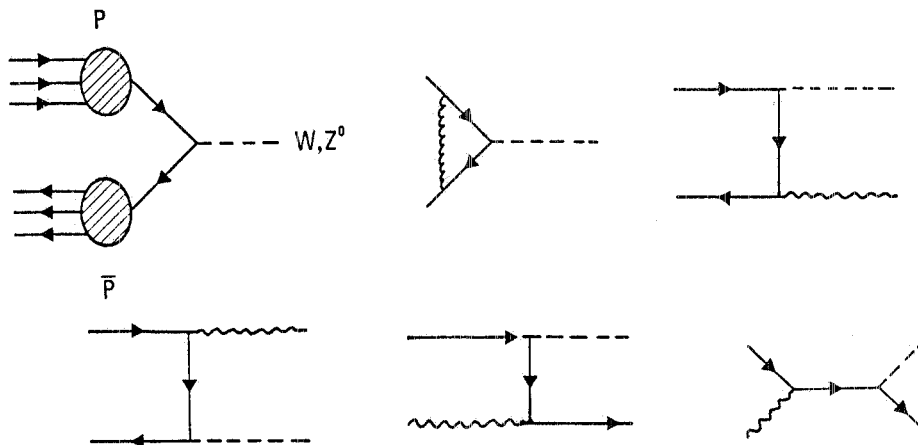


FIG. 1 Lowest order and order α_s diagrams relevant in W/Z^0 production. The wavy lines represent gluons.

The total cross section, including order α_s corrections, is often described by rescaling the lowest order formula:

$$\sigma^{W,Z} = K(Q^2, \tau) N_{W,Z} \int \frac{dx_1 dx_2}{x_1 x_2} \left\{ \left[H(x_1, x_2, Q^2) + (1 \leftrightarrow 2) \right] \delta\left(1 - \frac{\tau}{x_1 x_2}\right) \right\} \quad \text{where } Q = M_{W,Z} \quad (2)$$

$K(Q^2, \tau)$ is a very mild function of τ and Q in the range covered by experiments. At fixed target energies K is dangerously big for a genuine "perturbative" correction, $K \sim 1.8 + 2.0$, and all orders resummation techniques must be invoked in an attempt to control the perturbative series⁽³⁾. At Collider energies $K \sim 1.3 + 1.4$ and the total cross section can be predicted with a smaller theoretical uncertainty. By writing $K = 1 + \epsilon + O(\epsilon^2)$ we expect $O(\epsilon^2) \simeq 15\%$.

Other sources of theoretical uncertainties are:

- i) the choice of the parton densities: in W/Z^0 production at $\sqrt{s} = 540\text{--}630$ GeV the total cross section is dominated by the quark-antiquark annihilation process and we probe the parton densities in a range of $x_{1,2} \sim \sqrt{\tau} \sim 0.15$ where valence quark distributions are very well known from lower energies deep inelastic experiments. The theoretical error due to the choice of the parton densities is then rather small.
- ii) The scale P^2 appearing in the parton distributions and in α_s and

the value of Λ : different choices of P^2 in the parton distributions are compensated (at order α_s) by a redefinition of $f_{q,g}(z)$ in Eq. (1). More important is choice of the scale (and/or of Λ) in α_s . One could argue that the relevant scale could be smaller than the intermediate vector boson mass (for a more detailed discussion see Ref. (4)):

$$\langle q_T \rangle^2 \lesssim P^2 \lesssim M_{W,Z}^2 \quad (3)$$

where $\langle q_T \rangle$ is the average transverse momentum ($\langle q_T \rangle \simeq 7+8$ GeV). Since $q_T \ll M_{W,Z}$ the choice of the scale sensibly modify the results. In Table I I report the predicted values for the total W/Z^0 production cross section at $\sqrt{S} = 540-630$ GeV together with an estimate of the theoretical error coming from the uncertainties discussed above^(4,5,6). Notice that the relative error for $\sigma^{W^+W^-} / \sigma^{Z^0}$ (which is an important quantity for the evaluation of the total Z^0 width⁽⁷⁾) is much smaller ($\lesssim 10\%$) than the relative error on the cross section since most of the theoretical uncertainties cancel in the ratio. Another quantity which can be predicted with a small error is the ratio of production cross section at different energies. We expect

$$\frac{\sigma(\sqrt{S} = 630 \text{ GeV})}{\sigma(\sqrt{S} = 540 \text{ GeV})} \simeq 1.25$$

both for W and Z^0 production. From Table I, assuming for the branching ratios:

$$B(W \rightarrow e\nu) = 0.089 \quad B(Z^0 \rightarrow e^+e^-) = 0.032$$

TABLE I

$\sigma^{W^+W^-}$ (nb)	σ^{Z^0} (nb)	$\sigma^{W^+W^-} / \sigma^{Z^0}$	\sqrt{S} (GeV)
$4.2^{+1.3}_{-0.6}$	$1.3^{+0.4}_{-0.2}$	3.3 ± 0.2	540
$5.3^{+1.6}_{-0.9}$	$1.6^{+0.5}_{-0.3}$		630

one obtains the figures reported in Table II where for comparison the experimental results are also given. Theoretical predictions and experimental results are in agreement within the errors. Without the order α_s corrections all the theoretical values should be lowered by $\sim 35\%$. They would then be barely compatible with experimental results. I would like to add a comment: of the existing computations take seriously only those which into account $O(\alpha_s)$ corrections and do not derive total cross section by integrating numerically $d\sigma/dq_T$ (q_T = transverse momentum) after having introduced uncontrolled approximations in the resummation of soft gluon effects at all orders in perturbation theory (see next subsection).

$(B(W \rightarrow e\nu)\sigma^W)_{th} (pb)$	UA1	UA2	$\sqrt{S} (GeV)$
370^{+110}_{-60}	$530^{+80^{+90}}$ (590)	$500^{+100^{+80}}$	540
470^{+140}_{-80}	$480^{+40^{+80}}$	$540^{+70^{+90}}$	630
$(B\sigma^{Z^0})_{th} (pb)$	UA1	UA2	
42^{+12}_{-6}	$41^{+21^{+7}}$	$101^{+37^{+15}}$	540
51^{+16}_{-9}	$64^{+21^{+10}}$	$56^{+20^{+9}}$	630

TABLE II - Comparison of theoretical predictions and experimental results for the total cross section times the branching ratio. The UA2 results at $\sqrt{S} = 540$ GeV (Ref. (8)) have been corrected after a new evaluation of the integrated luminosity (Ref. (9)). The UA1 data for W production are uncorrected; the figure in bracket refers to the corrected value at $\sqrt{S} = 540$ GeV (Refs. (10,11)). The quoted UA1 result at $\sqrt{S} = 630$ GeV for Z^0 production refers to the channel $Z^0 \rightarrow \mu^+ \mu^-$. All the others results for Z^0 refers to $Z^0 \rightarrow e^+ e^-$.

2.2 Transverse Momentum Distribution

To get predictions for the boson transverse momentum distribution all orders effects need to be taken into account in the region of small transverse momenta, $\Lambda \ll q_T \ll Q \sim M_{W,Z}$, because of the presence of large terms of order:

$$\frac{1}{q_T^2} \alpha_s^n (q_T^2) \ln^m(Q^2/q_T^2) \quad m \leq 2n-1$$

The resummation to all order of these terms, first attempted by Dokshitzer-Diakonov-Troyan (DDT)⁽¹²⁾, Parisi and Petronzio⁽¹³⁾, Curci et al.⁽¹⁴⁾, has been extended beyond the double leading logarithmic approximation by Collins and Soper⁽¹⁵⁾. More recently⁽⁴⁾ an analytic expression for $d\sigma/dq_T$ has been presented satisfying the following requirements:

- a) at large q_T the correct behavior resulting from the recoil against one parton⁽¹⁶⁾ is automatically reproduced
- b) in the region $q_T \ll Q = M_{W,Z}$ the soft gluon exponentiation is performed at the leading and next to leading double logarithmic accuracy^(12,13,14,15)
- c) upon integration over q_T the known perturbative results for the total cross section (and $d\sigma/dy$)^(1,2,17) are obtained including terms of order α_s (which give rise to the "K-factors")
- d) all cross sections are expressed in terms of quark distributions which are precisely specified beyond the leading order.

A different approach has been followed by the authors of Ref. (18). The approach of Ref. (4,5) can be augmented by higher order terms when these will become available. Actually one can take advantage of the existing $O(\alpha_s^2)$ corrections to the double logarithmic approximation first derived in Ref. (19) and recently confirmed by Davies and Stirling⁽²⁰⁾ by using the results of Ref. (21).

The fact that the resummation is necessary is demonstrated in Fig. 2 where a comparison of the all order resummed expression for

$$\left. \frac{d\sigma}{dq_T dy} \right|_{y=0}$$

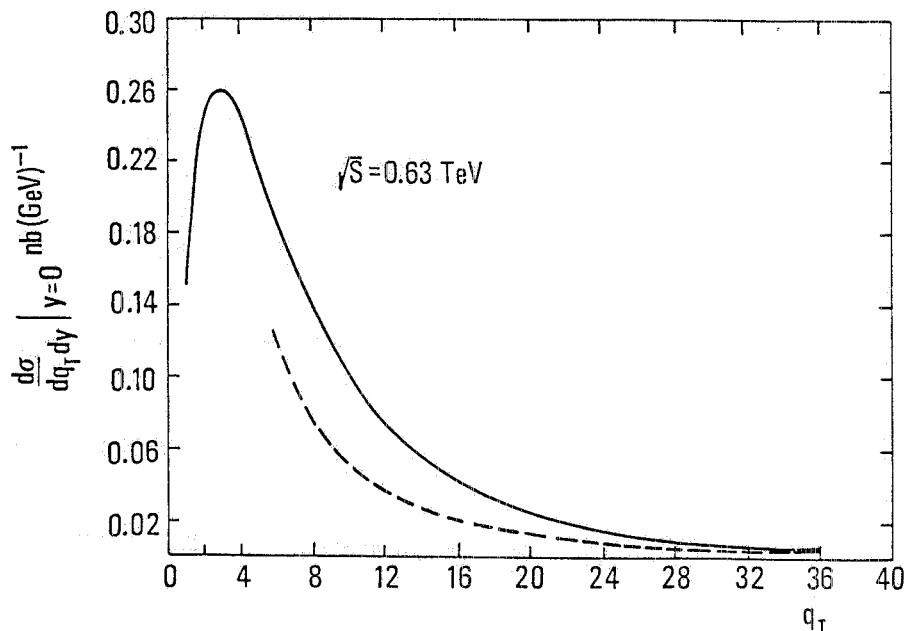


FIG. 2 - Comparison of the resummed expression for $(d\sigma/dq_T dy)|_{y=0}$ (solid line) with the first order perturbative expression (dashed line) at $\sqrt{S}=630$ GeV.

with the first order perturbative expression is presented. From this figure we see that the perturbative tail is an adequate description of the q_T distribution only for $q_T \gtrsim 25-30$ GeV. In Figg. 3a and 3b a comparison between the theoretical predictions for the transverse momentum distribution of the W and the more recent data from the UA1 and UA2 collaboration is reported. The agreement is excellent. However I want to remind here that the predictions for the q_T distribution are also affected by several uncertainties. In the present case the main source of error comes from the choice of the value of Λ in the running coupling constant. This is illustrated in Fig. 4 where I report two different curves (taken from Ref. (4)) corresponding to different values of Λ and of the parton parametrizations. The difference between the two curves is mostly due to the difference in the value of Λ ($\Lambda=0.2$ or $\Lambda=0.4$ GeV). We notice here that the vector boson transverse momentum distribution determines the transverse momentum of the final electron when the decay $W \rightarrow e\nu$ occurs and hence the values of the W mass extracted from the lepton spectrum. The uncertainties due to lack

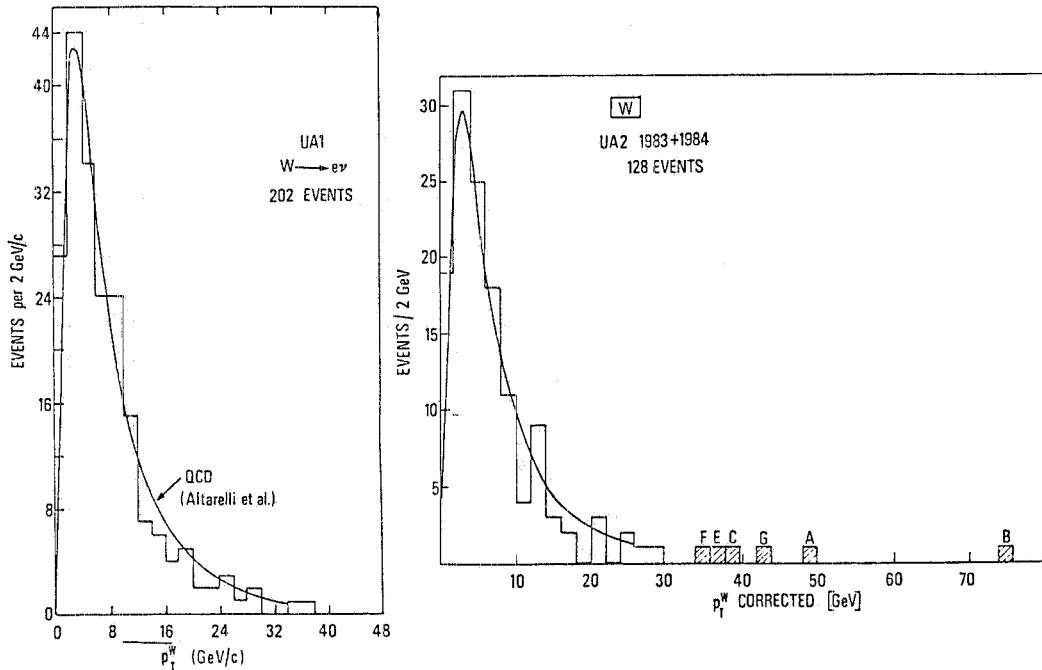


FIG. 3a/b p_T^W distributions of the W reported at this Meeting by the UA1 (11) and the UA2 (22) collaborations plotted against the theoretical predictions from Ref. (4).

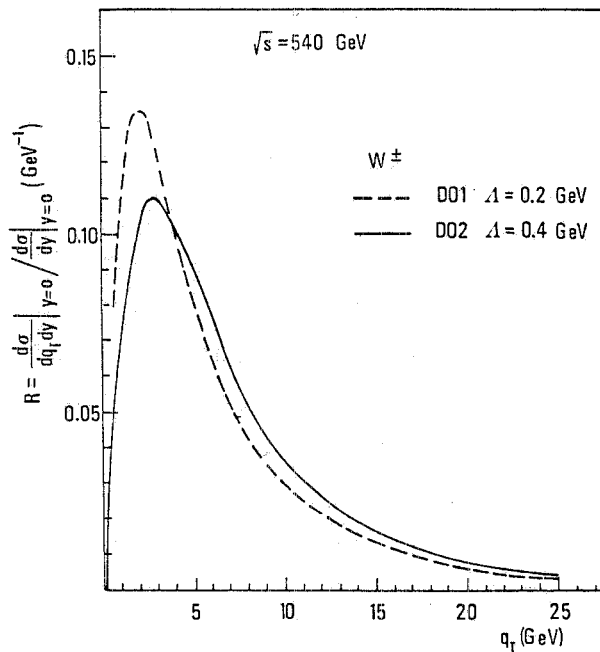


FIG. 4 - $(d\sigma / dq_T dy) / (d\sigma / dy)$ versus q_T at rapidity $y=0$ for W production at $\sqrt{s}=540$ GeV. The dashed lines uses the Duke-Owens parametrization (23) with $\Delta=0.2$ GeV whilst the solid line corresponds to the parametrization with $\Delta=0.4$ GeV.

of precise knowledge of the input parameters should be taken into account as a systematic error in the experimental evaluation of the W mass from the electron spectrum (cfr. Ref. (9)).

2.3 Quantities Determined by the Large Transverse Momentum Tail of the Distribution

In this subsection I will focus my attention on two quantities which, at large energies, are dominated by the perturbative tail of the q_T distribution.

a) Let us define $\pi(q_T)$ as the probability of W/Z^0 production with a transverse momentum larger than a given value q_T ^(f):

$$\pi(q_T) = \frac{\int_{q_T}^{q_T^{\max}} \left(\frac{d\sigma}{dq_T}\right) dq_T}{\int_0^{q_T^{\max}} \left(\frac{d\sigma}{dq_T}\right) dq_T} \quad (6)$$

In W/Z^0 production, for q_T large enough ($q_T \gtrsim 25-30$ GeV; cfr the preceding section) $\pi(q_T)$ is essentially determined by the first order perturbative transverse momentum tail.

The interest for $\pi(q_T)$ stems from the fact that signals of new physics are expected to show up at large q_T . A precise knowledge of $\pi(q_T)$ provides an estimate of the background at large q_T due to the physics of the Standard model. In fact Z^0 events at large q_T can appear as monojets if the decay $Z^0 \rightarrow \bar{\nu}_i \nu_i$ occurs and similarly W events at large q_T would produce events with one electron + jet + missing energy. $\pi(q_T)$ was evaluated in Refs. (5,24). The figures presented in Table III are from Ref. (5). The errors include the uncertainties on parton distributions, the scale in α_s and the value of Λ . In Ref. (5) also an estimate of the effects of the $O(\alpha_s^2)$ corrections (partially calculated

(f) Relative probabilities are better than absolute rates. From the probabilities one can more easily obtain the fraction of W/Z^0 events expected at large q_T from the total number of observed events (assuming that the experimental acceptance and efficiency are independent of q_T).

TABLE III

q_T	$\pi^W(q_T)\%$	$\pi^Z(q_T)\%$
25	$4.4^{+2.0}$	$5.1^{+2.5}$
30	$2.7^{+1.1}$	$3.2^{+1.3}$
35	$1.7^{+0.7}$	$2.0^{+0.8}$
40	$1.1^{+0.4}$	$1.4^{+0.5}$
45	$0.7^{+0.3}$	$0.9^{+0.3}$
50	$0.5^{+0.1}$	$0.6^{+0.2}$
55	$0.30^{+0.07}$	$0.40^{+0.10}$
60	$0.20^{+0.07}$	$0.25^{+0.10}$

q_T	$\pi^W(q_T)\%$	$\pi^Z(q_T)\%$
25	$5.4^{+2.3}$	$6.1^{+2.8}$
30	$3.5^{+1.3}$	$4.0^{+1.6}$
35	$2.3^{+0.8}$	$2.6^{+1.0}$
40	$1.5^{+0.5}$	$1.8^{+0.6}$
45	$1.0^{+0.3}$	$1.2^{+0.4}$
50	$0.7^{+0.2}$	$0.9^{+0.2}$
55	$0.50^{+0.15}$	$0.60^{+0.15}$
60	$0.30^{+0.09}$	$0.40^{+0.12}$

$\sqrt{s} = 540 \text{ GeV.}$

$\sqrt{s} = 630 \text{ GeV.}$

in Refs. (21)) was also given. From Table III, taking into account a factor 6 between $(Z^0 \rightarrow \bar{\nu}_i \nu_i)$ and $(Z^0 \rightarrow e^+ e^-)$ it follows that we expect at most 20% as many monojets with $q_T \geq 35 \text{ GeV}$ as observed $Z^0 \rightarrow e^+ e^-$ events.

b) Another relevant physical quantity is the average transverse momentum $\langle q_T \rangle$:

$$\langle q_T \rangle = \frac{\int_0^{q_T^{\max}} q_T \left(\frac{d\sigma}{dq_T} \right) dq_T}{\int_0^{q_T^{\max}} \left(\frac{d\sigma}{dq_T} \right) dq_T} \quad (7)$$

At Collider energies first order perturbative formulae can be used in an

efficient way to evaluate $\langle q_T \rangle$ (f). One obtains:

$$\langle q_T \rangle = 7 \pm 1 \text{ GeV} \quad \text{at} \quad \sqrt{S} = 540 \text{ GeV}$$

Within the theoretical error ($\sim 1 \text{ GeV}$) the inclusion of an intrinsic q_T does not effect in practice the result. The theoretical expectation in Eq. (7) agrees with the experimental results.

It is very interesting to compare results for Drell-Yan processes at fixed target and ISR energies with those obtained at Collider energies. The same formulae and input parameters (parton densities, Λ , ...) used for W/Z^0 production at $\sqrt{S} = 540$ and 630 GeV were used in Ref. (25) to compare theoretical predictions and experimental results for total cross sections and q_T distributions in Drell-Yan lepton pair production at low energies ($\sqrt{S} = 27+63 \text{ GeV}$). The agreement between theory and experiments is excellent (see Camilleri talk at this meeting). Here I will only report on the behavior of $\langle q_T \rangle$ as a function \sqrt{S} . Lowest order QCD predicts a linear rising of $\langle q_T \rangle$ with \sqrt{S} :

$$\langle q_T \rangle = \alpha_s h(\tau, Q) \sqrt{S} + \dots \quad (8)$$

h is a smooth function of τ and it depends logarithmically on $Q = \text{mass of the lepton pair}$. The dots indicate terms which are down by power of \sqrt{S} . Below ISR energies the effects of scaling violations and sub-asymptotic contributions from soft gluons significantly distort the linear behaviour of the average transverse momentum as a function of \sqrt{S} as shown in Fig. 5. The extrapolation of the linear slope of $\langle q_T \rangle$ at Collider energies leads to $\langle q_T \rangle \simeq 7+8 \text{ GeV}$ in good agreement with the observed value in W/Z^0 production, despite the fact one is comparing $p-p$ and $p-\bar{p}$, different values of \sqrt{s} and virtual photons with weak bosons.

(f) The value of $\langle q_T \rangle$ obtained by using the first order expression for $d\sigma/dq_T$ and the all orders resummed expression are perfectly consistent at $\sqrt{S} = 540$ or 630 GeV .

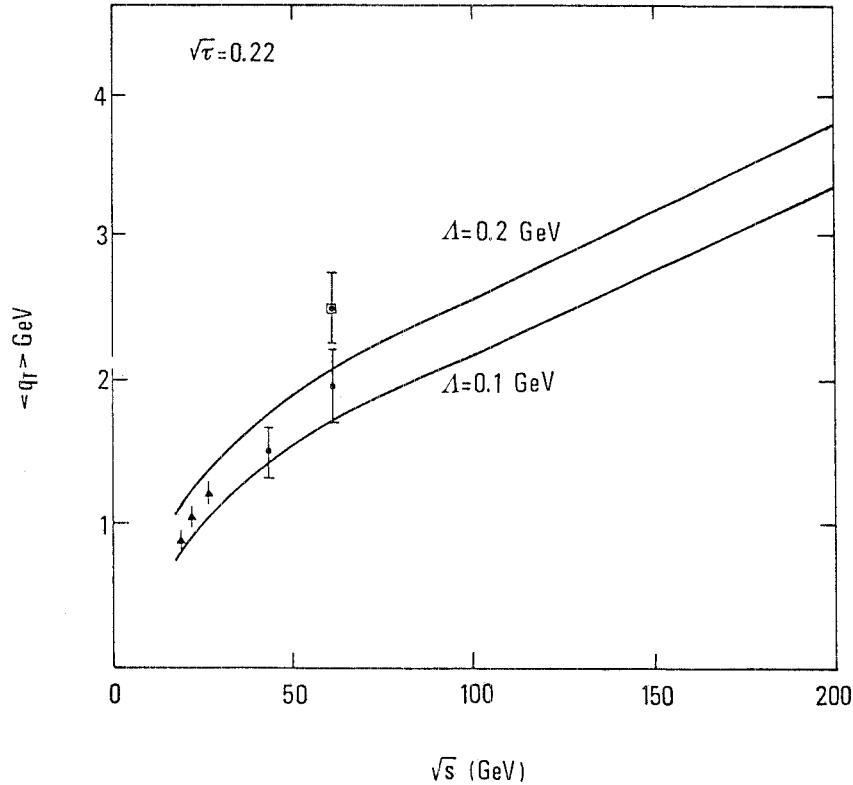


FIG. 5 - $\langle q_T \rangle$ versus \sqrt{s} at fixed $\sqrt{\tau} \simeq 0.22$. The data are from Ref. (26). The curves are the theoretical predictions for $\Delta = 0.1$ and $\Delta = 0.2$ GeV. No intrinsic q_T is included. At large values at \sqrt{s} $\langle q_T \rangle$ increases linearly in \sqrt{s} .

2.4 Transverse Energy Distribution

A correct treatment of the transverse energy (E_T) distribution is relevant not only for W/Z^0 production but also for the inclusive E_T distribution of jets. Preliminary results for the E_T distribution in W production were presented at this meeting by the UA1 and UA2 collaborations^(11,12). As it was the case for the transverse momentum distribution, all orders in perturbation theory must be taken into account at small values of E_T , ($E_T \ll M_{Z,W}$), because of the appearance of large logarithms. In the case of the transverse energy we expect a much harder distribution than in the q_T case since the emission of many soft gluons will give rise to events with a small total transverse momentum but a large energy as explained in Fig. 6. In Fig. 7 I compare

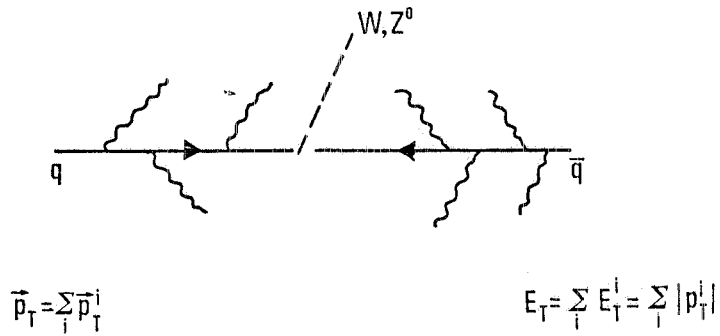


FIG. 6 - Emission of many soft gluons in W, Z^0 production. The total transverse energy E_T , being the sum of the absolute values of the transverse momenta of the gluons, is much larger than q_T since gluon momenta nearly compensate.

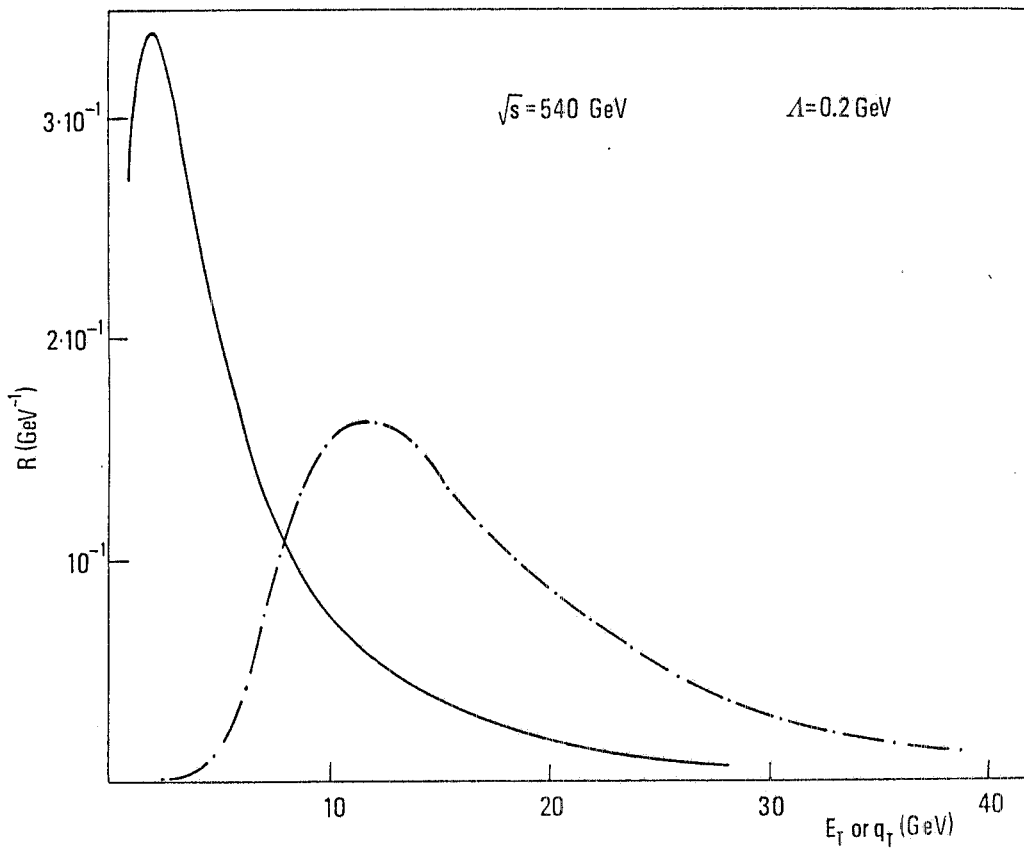


FIG. 7 - Comparison of the E_T distribution (dashed-dotted line) with the q_T distribution (solid line) in W production at $\sqrt{s} = 540 \text{ GeV}$.

the theoretical curves for E_T and q_T distributions, in W production, at $\sqrt{S}=540$ GeV.

Soft gluon emission from initial parton legs is also one of the mechanisms responsible for the difference of the $\langle E_T \rangle$, as measured in minimum bias events, with respect to the $\langle E_T \rangle$ of the so-called "underlying" events in two jets processes.

In practice the main difference between the transverse momentum and the transverse energy distributions in comparing theoretical predictions with experimental results arises because the E_T distribution (unlike the other) is heavily affected by parton hadronization and by the presence of the p and \bar{p} fragments as shown in Fig. 8. The effects of the p and \bar{p} fragments can be eventually reduced

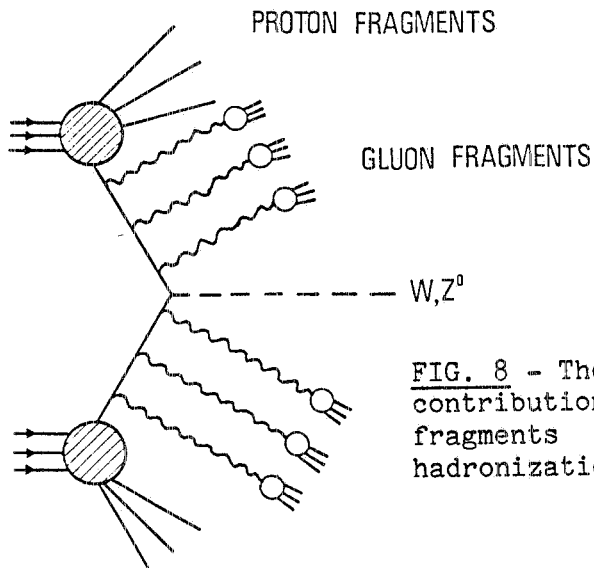


FIG. 8 - The E_T of the event get a substantial contribution from the proton (antiproton) fragments and it is modified by the hadronization of the emitted gluons.

by a suitable cutoff on the polar angle⁽²⁷⁾ (and energy) of the emitted particles.

Very recently an analytic expression for the E_T distribution was found⁽²⁸⁾, with the same positive features of the q_T distribution previously discussed. It has the form:

$$\frac{d\sigma^{W,Z}}{dE_T dy} = \frac{N_{W,Z}}{\pi} \int_0^\infty db b e^{S_R(b)} \left\{ H_1(b) \cos [bE_T - S_I(b)] - H_2(b) \sin [bE_T - S_I(b)] \right\} + Y(E_T) \quad (9)$$

where

$$S_{R,I}(b) = C_F \int_0^{q_T^{\max}} dq_T \left\{ \left[\frac{\alpha_s(q_T^2)}{2\pi} \frac{[4 \ln(Q^2/q_T^2) - 6]}{q_T} + O(\alpha_s^2) \right] (\cos(bq_T) - 1, \sin(bq_T)) \right\} \quad (10)$$

$q_T^{\max} = Q = M_{W,Z}$ when $E_T \leq Q$; $Y(E_T)$ is regular as $E_T \rightarrow 0$ and:

$$H_{1,2}(b) = \text{Im, Real} \int_0^{q_T^{\max}} dE_T e^{ibE_T} \left[H(x_1^0, x_2^0, E_T) + O(\alpha_s) \right] \quad (11)$$

where $O(\alpha_s)$ in Eq. (11) is a perturbatively computable function of $x_{1,2}^0$ ($x_{1,2}^0 = \sqrt{\tau} e^{\pm y}$). $H(x_1^0, x_2^0, E_T)$ is the appropriate bilinear combination of quark-antiquark distributions (cfr. Eq. (1)). As it was in the q_T case:

$$\int_0^{E_T^{\max}} \left(\frac{d\sigma}{dE_T} \right) dE_T = \sigma \quad (12)$$

where σ is the total production cross section including the first order correction ("K-factor"). The E_T distribution is more sensitive to the value of Λ than the q_T distribution (Fig. 9). Depending on Λ the maximum of the distribution ranges between $E_T \sim 7$ GeV and $E_T \sim 14$ GeV. This concludes the section on QCD effects in W/Z^0 production.

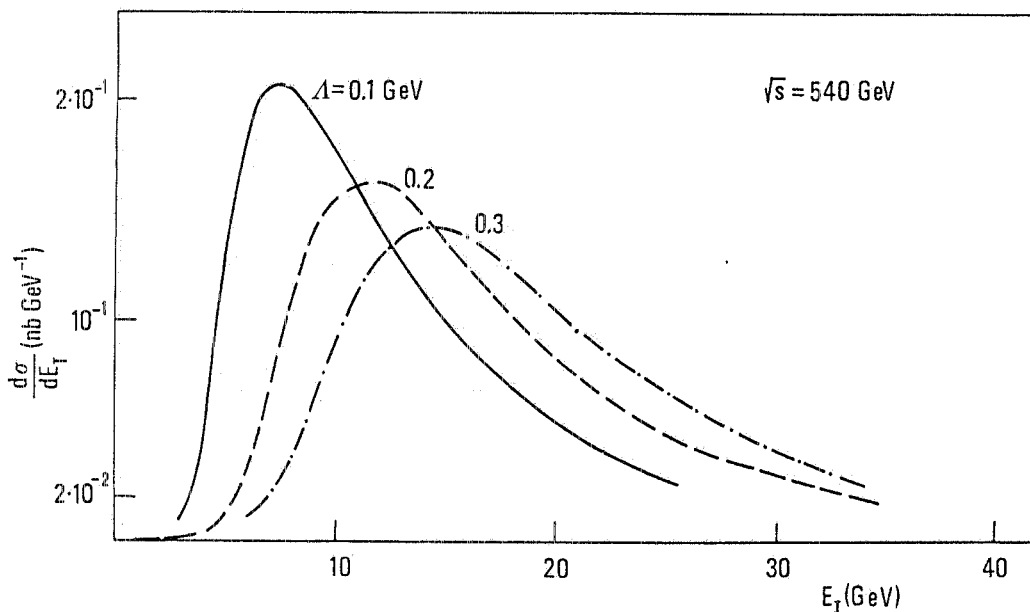


FIG. 9 - The Δ -dependence of the E_T distribution is shown in W production at $\sqrt{s}=540$ GeV. The curves correspond to $\Delta=0.1$ (dashed line), $\Delta=0.2$ (dashed line) and $\Delta=0.3$ GeV (dashed-dotted line).

3. JET PHYSICS AT THE CERN COLLIDER

This section is devoted to a discussion of the present status of the theory in jet physics and its comparison with experimental results.

We have seen in the preceding section that theory can, for most of the interesting physical quantities in W and Z^0 production, make quantitative predictions at a level of accuracy between 15% and 50%. The situation is certainly not that good in jet physics, although some of the problems from which present theoretical uncertainties originate will be probably solved in the next future with some theoretical effort.

A discussion of the theoretical uncertainties for inclusive jet cross sections will be the subject of the subsections 3.1 and 3.2. Finally in subsection 3.3 I will discuss some of the gluon effects that could be observed by experiments at the Collider.

3.1 Two Jet Cross Section

At the CERN Collider jets are observed by applying a trigger based on the total transverse energy of the events ($E_T = \sum_i E_T^i \geq E_T^{\text{Trigger}}$) or on a "two jets" and "single jet" trigger^(29,30). In two jets events the relevant parameter which measures the fraction of momentum carried by the incoming partons is $x_T = 2E_T/\sqrt{S}$. Typically:

$$0.07 \lesssim x_T \lesssim 0.5 \quad \text{at } \sqrt{S}=540 \text{ GeV}$$

Theoretical predictions for the cross section are based on the lowest order (α_s^2) parton cross section:

$$\frac{Ed^3\sigma}{d^3p} = \sum_{A,B} \int dx_1 dx_2 P_A(x_1, P^2) P_B(x_2, P^2) \delta(s+t+u) \quad (13)$$

$$\alpha_s^2(P^2) \sum_f \frac{|M_{AB \rightarrow f}|^2}{s}$$

$p_1 = x_1 P_1$ and $p_2 = x_2 P_2$ are the momenta of the incoming partons; the sum on A and B runs over different type of partons; s, t and u are the Mandelstam variables and P^2 is some (for the moment) unknown scale related to the transverse momentum of the final partons. $M_{AB \rightarrow f}$ is the invariant matrix element. Eq. (13) predicts the following fall off of $d\sigma/dq_T$ with q_T :

$$\frac{d\sigma}{dq_T^2} = \frac{f(x_T, \ln q_T^2)}{q_T^4} \quad (14)$$

In Eq. (13) the sum runs over all the possible parton subprocesses which can produce two jet events.

- a) $q + q \rightarrow q + q$
 - b) $g + g \rightarrow q + \bar{q}$
 - c) $q + \bar{q} \rightarrow g + g$
 - d) $g + g \rightarrow g + g$
 - e) $q + g \rightarrow q + g$
 - f) $q + \bar{q} \rightarrow q + \bar{q}$
- (15)

The cross section for the relevant subprocesses a) ... f) have been summarized in Ref. (31). The processes d) and e) dominate in the low q_T (x_T) region; at large q_T the dominant process is $q + \bar{q} \rightarrow q + \bar{q}$. This happens since valence quark distributions are much stiffer than gluon distributions. Processes a), b) and c) give a relatively small contribution in the whole q_T range. In Fig. 10 I report the trasverse q_T distribution

$$\left. \frac{d\sigma}{dq_T dy} \right|_{y=0}$$

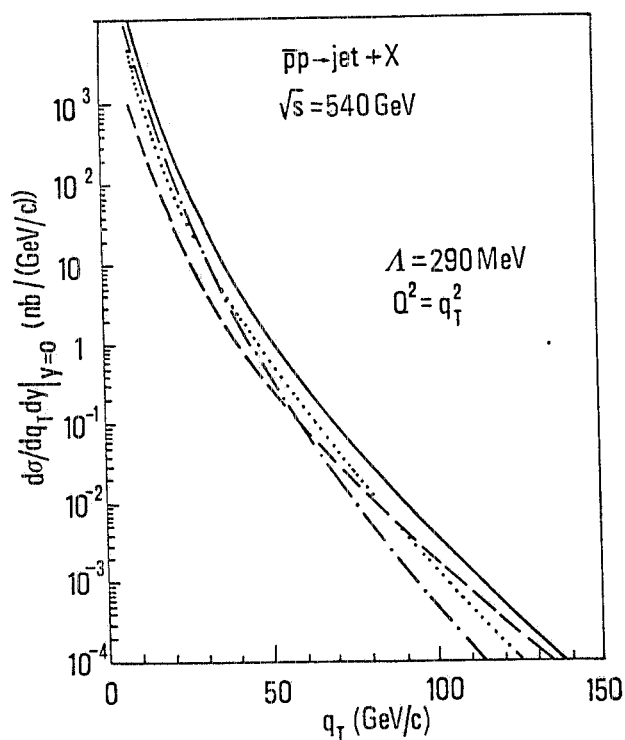


FIG. 10 - Differential cross section (solid line) at zero rapidity in pp collisions at $\sqrt{s}=540$ GeV according to the parton distributions of Ref.(32). The g-g (dot-dashed line) qg (dotted line) and qq (dashed line) are shown separately .

at $\sqrt{s}=540$ GeV obtained by using the parton parametrization of Ref. (31). The contribution from the processes d), e) and f) are shown separately. We see that for $q_T \lesssim 70-80$ GeV gluon initiated processes dominate the cross section. At different values of the center of mass energy \sqrt{s} , the gluon dominated region will change since the relevant

parameter is the (dimensionless) fraction of momentum of the incoming partons $x_T^{(f)}$. For this reason, in the low q_T region, the $gg \rightarrow gg$ contribution to the cross section will become more and more important than the $qg \rightarrow qg$ contribution as we increase the center of mass energy \sqrt{s} .

In Fig. 11 I report as an example the experimental results for

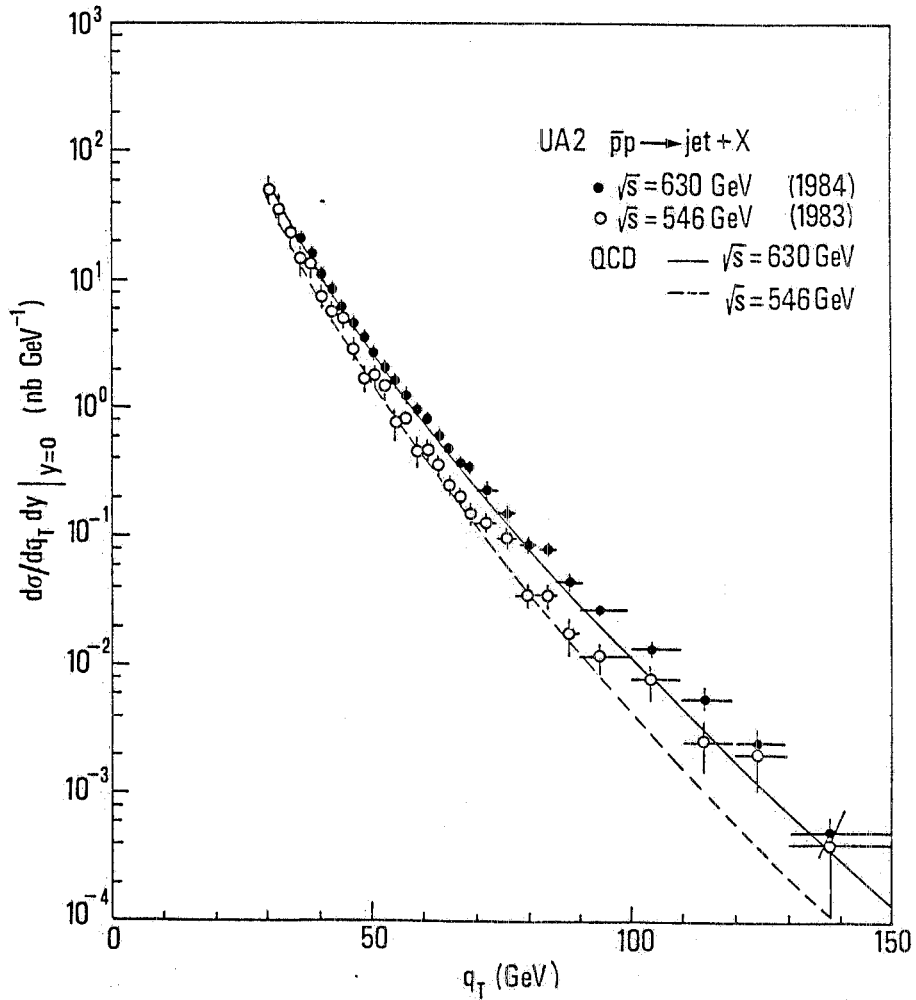


FIG. 11 - Comparison of the experimental data from Ref. (30) with lowest order theoretical predictions for the q_T distribution at zero rapidity.

(f) Scaling violations may have some small effect at energies larger than CERN Collider.

$d\sigma/dq_T$ at $\sqrt{S}=540$ GeV and $\sqrt{S}=630$ GeV⁽³⁰⁾ compared to theoretical predictions obtained by using the parton parametrizations of Refs. (32). The agreement is quite spectacular given that the q_T distribution falls of several orders of magnitude in the range of q_T covered by experiments. When comparing data and theoretical predictions we have to taken into account that there is an experimental uncertainty on the cross section of $\sim 40-60\%$ coming from the systematic errors in measuring jet energies and that the theoretical error is of about a factor 2. The theoretical uncertainties in the evaluation of the two jets cross section will be the subject of subsection 3.2.

3.2 Uncertainties in the Cross Section

I divide the sources of theoretical uncertainties in two groups:

a) The value of Λ in the running coupling constant and the choice of the parton densities.

b) The scale in α_s (and in the non scaling parton densities) and higher order corrections.

a) It is a very simple exercise to show how large is the effect of choosing different values of Λ , for the parton cross section (we expect a large effects since $d\sigma/dq_T \sim \alpha_s^2$). Assuming that the scale in α_s is $q_T^2/4$ we find:

$$\left[\frac{\alpha_s(q_T=20 \text{ GeV}, \Lambda=0.5 \text{ GeV})}{\alpha_s(q_T=20 \text{ GeV}, \Lambda=0.1 \text{ GeV})} \right]^2 \sim 2.4 \quad (16)$$

$$\left[\frac{\alpha_s(q_T=150 \text{ GeV}, \Lambda=0.5 \text{ GeV})}{\alpha_s(q_T=150 \text{ GeV}, \Lambda=0.1 \text{ GeV})} \right]^2 \sim 1.7$$

A related problem is the choice of the parton parametrization. The parton distributions one can buy on the market (the gluon distribution in particular) are strongly correlated to the value of Λ that has been

used to fit the data. Thus is not correct, in evaluating the theoretical error, to change Λ , for a given parametrization, in an arbitrary way.

Our ignorance of the gluon distribution from deep inelastic scattering does not lead, contrary to naïve expectations, to a large uncertainty in the cross section at present Collider energies (where the typical scale of jet events is $P^2 \sim 2000 \text{ GeV}^2$). Despite of large differences at low scales, different gluon parametrizations are practically identical in the region where they dominate the cross section. This comes because gluons are mostly generated by valence quarks at lower scales and higher values of the Bjorken variable x , where quarks are well measured from deep inelastic experiments. For the same reason we may expect larger and larger uncertainties as we proceed in the very large q_T region: also if there valence quarks dominate, their distribution is determined by quark distributions at lower P^2 and larger x where structure functions are badly measured.

b) A theoretical issue, also related to the value of Λ , is the choice of P (cfr. Eq. (13)), the scale at which parton densities and the running coupling constant must be evaluated. If the complete order α_s^3 were available, one could fix the scale by minimizing higher order corrections. In the absence of this computation⁽³³⁾ one can make a guess based on the only fragment of the $O(\alpha_s^3)$ corrections presently available⁽³⁴⁾. That example shows that the corrections can be quite sizeable ($\gtrsim 100\%$) and that the "K-factor"^(f):

$$K = \frac{\frac{d\sigma}{dq_T} \alpha_s^3}{\frac{d\sigma}{dq_T} \alpha_s^2} \quad (17)$$

(f) $d\sigma^3/dq_T$ ($d\sigma^2/dq_T$) is the q_T distribution up to (and including) the order α_s^3 (α_s^2) terms.

is remarkably constant in q_T , thus not affecting the shape of the distribution (Fig. (12)). The computation of Ref. (34) and (35) also

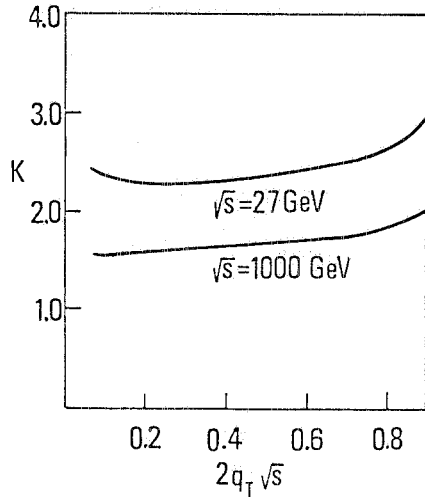


FIG. 12 - The "K-factor" is reported at two different values of the center of mass energy $\sqrt{s}=27$ GeV and $\sqrt{s}=1$ TeV. The curves, referring to the process $q_i+q_j \rightarrow J+X$, $i \neq j$, are from Ref. (34).

suggests that the appropriate scale is $P^2=q_T^2/2$: with this choice $O(\alpha_s^3)$ corrections are reduced to $\sim 20\%$ throughout most of the range in q_T . Will really the $O(\alpha_s^3)$ computation reduce the theoretical uncertainty? We have to distinguish the low x_T and large x_T regions: in the former region, since the main problems come from the choice of Λ and of the scale P in α_s , next order will certainly help. On the contrary the knowledge of $O(\alpha_s^3)$ terms will probably not help very much in the large x_T region.

My conclusion is that the qualitative agreement between theoretical predictions and experimental results is a great success of perturbative QCD and that the computation of the $O(\alpha_s^3)$ corrections, together with better experimental measurements will probably put this agreement on a more quantitative basis.

3.3 Gluon Effects in Jet Physics

As we have seen in subsection 3.1, the low x_T region is an ideal place to study gluon jets. At Tevatron energies there will be a larger kinematical (and experimentally accessible) region completely dominated by gluon jets.

Perturbative QCD predicts different longitudinal (z) and

transverse (p_T) distributions, with respect to the jet axis, for gluon and quark jets. In fact, because of colour factors, the gluon fragments more easily thus giving a softer and fatter jet than in the quark case. I report (Fig. 13) as an example the predicted z distributions for gluon and quark jets obtained by using the Webber Monte Carlo⁽³⁵⁾. The experimental situation is however more confused. A very interesting study of jet fragmentation properties have been presented at this meeting by the UA1 Collaboration⁽³⁶⁾. However, we still do not see clear experimental evidence of the difference between quark and gluon jets from the Cern Collider results.

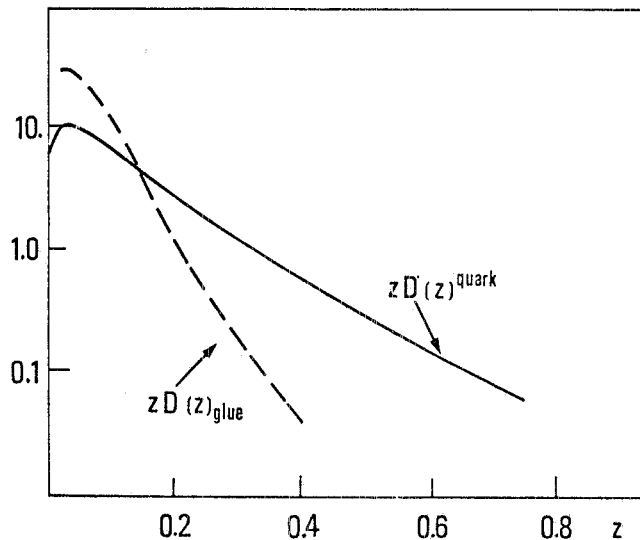


FIG. 13 - Theoretical predictions for the gluon (dashed line) and quark (solid line) jet longitudinal momentum distributions.

An interesting observation, concerning gluon effects in jet physics, has been recently done by M. Greco⁽³⁷⁾. If one considers the jet-jet system as a whole, the q_T distribution of this system, relatively to the beam axis, will be determined (at small q_T) by the emission of soft partons accompanying the two almost back-to-back jets. The Sudakov form factors, which regulate the q_T distribution, will differ strongly whether the incoming partons are quarks or gluons. In Fig. 14 I report the q_T distribution of the jet-jet system: the full line refers to the distribution obtained for gluon-gluon scattering

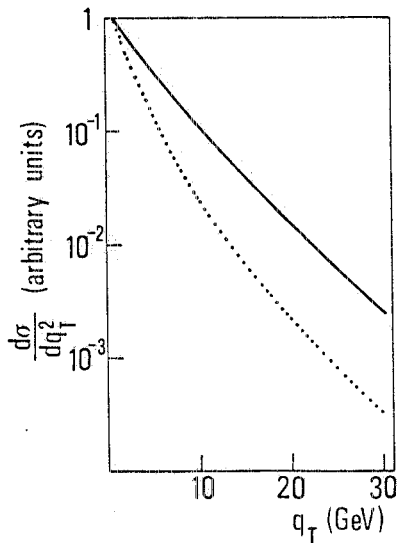


FIG. 14 - Transverse momentum distribution of the jet-jet system. The gluon distribution function (solid line) can be compared to the curve one obtains by putting $C_A = C_F = 4/3$, as in the quark case (dotted line).

processes. The dotted line is obtained by putting the gluon Sudakov form factor equal to the quark one ($C_A = 3 \rightarrow C_F = \frac{4}{3}$). The difference of the two distributions is mainly given by the effects of the three gluon coupling. A more accurate analysis of the separation of the two curves taking into account all the theoretical uncertainties (parton distribution, Λ , ..) is still missing. The same soft radiation from initial legs will also probably carry in better agreement the experimental results for the q_T^{out} distribution in two jet events (reported by F. Pastore at this meeting) with theoretical predictions (Fig. (15)). I have a final comment on the first attempts that have been made by the UA1 and UA2 collaborations in order to estimate the running coupling constant from the ratio

$$R = \frac{\sigma_{\text{3 jets}}}{\sigma_{\text{2 jets}}} \quad (18)$$

For a given definition of what is a two jets or a three jet event this is a very well defined experimental quantity. Caution must be used however in order to extract the value of the coupling constant by comparing R with theoretical predictions. Let me recall what happens in e^+e^- annihilation into jets, a case for which higher order corrections have been completely computed. In that case one was able to define a three jet cross sections:

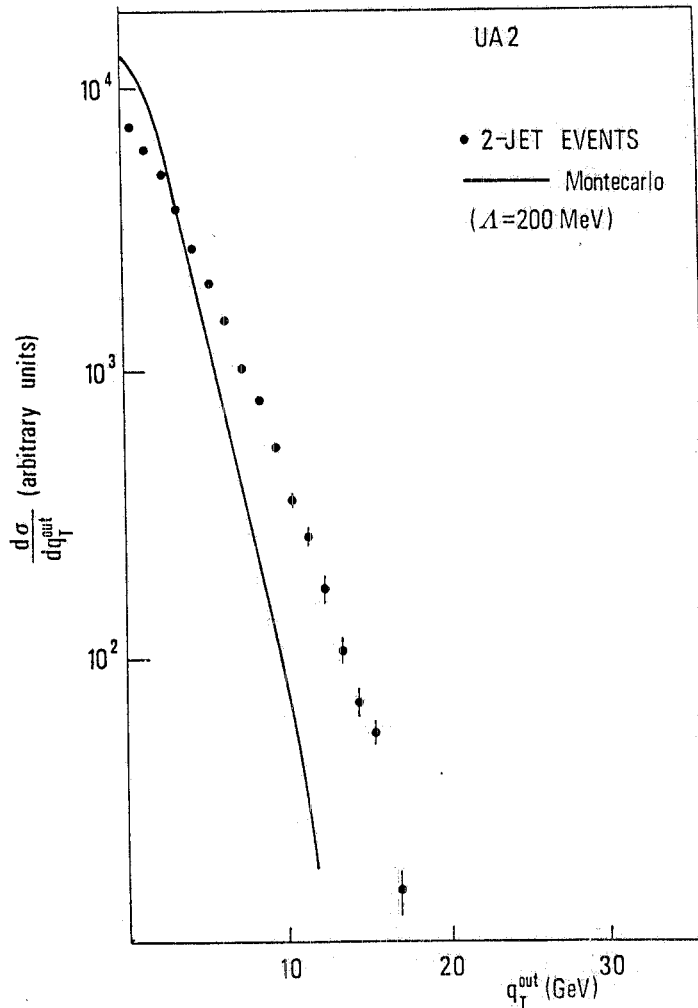


FIG. 15 - q_T^{out} distribution in two jet events compared with the results of a numerical simulation. The theoretical curve is much steeper than the data. Soft gluon emission may be a remedy to this difference.

$$\begin{aligned} \sigma(e^+e^- \rightarrow 3j) = & \sigma(e^+e^- \rightarrow 3j) \alpha_s + \sigma(e^+e^- \rightarrow 3j) \alpha_s^2 \\ & + \delta\sigma(e^+e^- \rightarrow 4j) \alpha_s^2 \end{aligned} \quad (19)$$

The first term on the r.h.s. of Eq. (19) is the lowest order ($O(\alpha_s)$) three jet cross section. The second term is given by the $O(\alpha_s^2)$ terms from virtual diagrams. The last term is the contribution from the four jet cross section when four jets appear as three jets because of the algorithm by which they are defined. It turned out that, at Petra

energies, the theoretical evaluation of the three jets cross section is strongly affected, because of higher order terms, by the definition of what is a jet and by the process of parton hadronization. The effects of higher order corrections are not known in jet physics and we cannot rely on (more or less educated) guesses that have been done, without any solid theoretical basis, on the size of these higher order terms⁽³⁸⁾.

ACKNOWLEDGMENTES

I thank G. Altarelli, P. Bagnaia, R.K. Ellis, M. Greco and L. Mapelli for usefull discussions.

REFERENCES

- (1) Altarelli, G., Ellis, R.K. and Martinelli, G., Nucl. Phys. B143, 521 (1978); (E) B196, 544 (1978; B157, 461 (1979).
- (2) Kubar-Andrè, J. and Paige, F.E., Phys. Rev. D19, 221 (1979).
- (3) Parisi, G., Phys. Letters 90B, 295 (1980); Curci, G. and Greco, M., Phys. Letters 92B, 175 (1980).
- (4) Altarelli, G. Ellis, R.K., Greco, M. and Martinelli, G., Nucl. Phys. B246, 12 (1984).
- (5) Altarelli, G., Ellis, R.K. and Martinelli, G., CERN-TH.4015/84 and Fermilab-Pub-84/107-T (1984) to appear in Zeit. für Physik C.
- (6) Chiappetta, P. and Perrottet, M., private communication.
- (7) Cabibbo, N., Proc. 3rd $\bar{p}p$ Workshop, Rome ed. by C. Bacci and G. Salvini, (1983).
- (8) UA2 Collaboration, presented by Schacher, J., Proc. 4th $\bar{p}p$ Workshop, Bern (1984).
- (9) UA2 Collaboration, presented by L. Mapelli at this Workshop.
- (10) UA1 Collaboration, presented by Rubbia, C., Proc. 4th $\bar{p}p$ Workshop, Bern (1984).
- (11) UA1 Collaboration, presented by Levy, M., at this Workshop.
- (12) Dokshitzer, Yu.L., Dyakonov, D.I. and Troyan, S.I., Phys. Letters 78B, 290 (1978); Phys. Rep. 58, 269 (1980).
- (13) Parisi, G. and Petronzio, R., Nucl. Phys. B154, 427 (1979).

- (14) Curci, G., Greco M. and Srivastava, Y.N., Phys. Rev. Letters 43, 434 (1979); Nucl. Phys. B159, 451 (1979).
- (15) Chao, S.C. and Soper, D.E., Nucl. Phys. B214, 405 (1983); Chao, S.C., Soper, D.E. and Collins, J.C., Nucl. Phys. B214, 513 (1983).
- (16) Altarelli, G., Parisi, G. and Petronzio, R., Phys. Letters 76B, 351 and 356 (1978); Fritzsche, H. and Minkowsky, P., Phys. Letters 74B, 384 (1978); Kajantie, K. and Raitio, R., Nucl. Phys. B139, 72 (1978); Halzen, F. and Scott, D.M., Phys. Rev. D18, 3378 (1978).
- (17) Kubar Andrè, G. Le Bellac, M., Meunier, J.L. and Plaut, G., Nucl. Phys. B175, 251 (1980).
- (18) Halzen, F., Martin, A.D. and Scott, D.M., Phys. Rev. D25, 754 (1982).
- (19) Kodaira, J. and Trentadue, L., Phys. Letters 112B, 66 (1982); 123B, 335 (1983).
- (20) Davies, C.T.H. and Stirling, W.J., CERN-TH.3853 (1984).
- (21) Ellis, R.K., Martinelli, G. and Petronzio, R., Nucl. Phys. B211, 106 (1983).
- (22) UA2 Collaboration, presented by Plothw-Besch H. at this Workshop.
- (23) Duke, D.W. and Owens, J.F., Phys. Rev. D30, 49 (1984).
- (24) Aurenche, P. and Kinnunen, R., LAPP-TH-108 (1984); Bellestero, A. and Passarino, G., preprint Univ. Turin IFTT-435 (1984).
- (25) Altarelli, G., Ellis, R.K. and Martinelli, G., CERN-TH-4049 (1984).
- (26) Angelis A.L.S. et al., CMOR Coll., CERN-EP 128/84 To be published in Phys. Letters; Antreasyan, D. et al., Phys. Rev. Letters 45, 863 (1980); 47, 12 (1981); 48, 302 (1982); Ito, A.S. et al., Phys. Rev. D23, 604 (1981).
- (27) Davies C.T.H. and Webber B.R., Z. Phys. C24, 133 (1984).
- (28) Altarelli, G., Martinelli, G. and Rapuano F. in preparation.
- (29) UA1 Collaboration, presented at this Meeting by Buckley, E.J.
- (30) UA2 Collaboration, presented at this Meeting by Pastore, F.
- (31) Owens, J.F., Reya, E. and Glück M., Phys. Rev. D18, 1501 (1978).
- (32) Eichten, E. Hinchliffe, I., Lane, K. and Quigg, C., Rev. of Mod. Physics 54, 579 (1984).

- (33) The result of the complete $O(\alpha_s^3)$ corrections will be hopefully available in the next future; Ellis, R.K. private communication.
- (34) Ellis, R.K., Furman, M.A., Haber, H.E. and Hinchliffe, I., Nucl. Phys. B137, 397 (1980).
- (35) Marchesini, G. and Webber, B.R., Nucl. Phys. B238, 1 (1984);
Webber, B.R., Nucl. Phys. B238, 492 (1984).
- (36) UA1 Collaboration, presented at this Meeting by H.Ghez.
- (37) Greco, M., Z. Phys. C26, 567 (1985).
- (38) Antoniou, N.G. et al., Phys. Letters 128B, 257 (1983).